

# Using Computational Fluid Dynamics Software to Estimate Circulation Time Distributions in Bioreactors

Kyle M. Davidson,<sup>†</sup> Shrinivasan Sushil,<sup>†</sup> Charles D. Eggleton,<sup>\*,†</sup> and Mark R. Marten<sup>\*,‡</sup>

Department of Mechanical Engineering and Department of Chemical and Biochemical Engineering, 1000 Hilltop Circle, University of Maryland, Baltimore County (UMBC), Baltimore, Maryland 21250

Nonideal mixing in many fermentation processes can lead to concentration gradients in nutrients, oxygen, and pH, among others. These gradients are likely to influence cellular behavior, growth, or yield of the fermentation process. Frequency of exposure to these gradients can be defined by the circulation time distribution (CTD). There are few examples of CTDs in the literature, and experimental determination of CTD is at best a challenging task. The goal in this study was to determine whether computational fluid dynamics (CFD) software (FLUENT 4 and MixSim) could be used to characterize the CTD in a single-impeller mixing tank. To accomplish this, CFD software was used to simulate flow fields in three different mixing tanks by meshing the tanks with a grid of elements and solving the Navier–Stokes equations using the  $\kappa$ - $\epsilon$  turbulence model. Tracer particles were released from a reference zone within the simulated flow fields, particle trajectories were simulated for 30 s, and the time taken for these tracer particles to return to the reference zone was calculated. CTDs determined by experimental measurement, which showed distinct features (log-normal, bimodal, and unimodal), were compared with CTDs determined using CFD simulation. Reproducing the signal processing procedures used in each of the experiments, CFD simulations captured the characteristic features of the experimentally measured CTDs. The CFD data suggests new signal processing procedures that predict unimodal CTDs for all three tanks.

## Introduction

Less-than-ideal mixing in large-scale fermentors can lead to concentration gradients in both oxygen and nutrients (1). For example, gradients in limiting nutrient can occur during fed-batch operation, when bulk mixing occurs more slowly than cellular consumption of the added nutrient. When this situation arises, the majority of the added nutrient will be consumed in a small region of the tank (“feed zone” (2)) near the nutrient addition port (Figure 1a). In other cases, gradients in oxygen can occur when the viscosity of fermentation broth is high (as a result of secreted polymers or filamentous cell morphology). Because viscous fermentation broth is typically shear thinning, oxygen mass transfer will predominantly take place near the impellers (Figure 1b) (3). Many industrial fermentations are operated with viscous broths (4), and feed zones have been shown to occur not only in viscous fungal fermentations but also in bacterial fermentations as well (5). The implication is that concentration gradients not only are possible but may be prevalent in a significant number of industrial fermentation processes.

When concentration gradients arise, it is likely that productivity of a microbial culture will depend on the frequency and duration of exposure to the nutrient- or

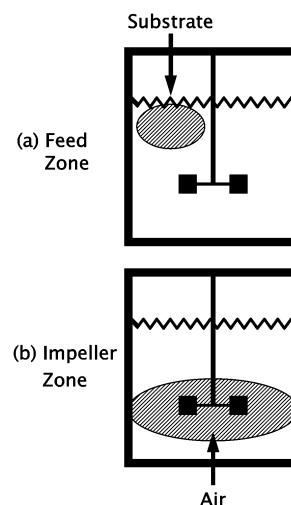


**Figure 1.** Schematic illustration showing possible concentration gradients in (a) substrate and (b) oxygen, resulting from inadequate mixing or high viscosity fermentation broth.

oxygen-rich portion of the fermentor (6). These frequencies and residence times are controlled by macro mixing and can be quantified by the circulation time distribution (CTD) (1, 5, 7). Circulation time ( $t_c$ ) is defined as the time between consecutive passages of a particular cell through the nutrient or oxygen rich zone. The CTD then, is a function describing the frequency of all possible  $t_c$ 's. Thus, to rigorously study cellular responses to less-than-ideal mixing requires knowledge of the CTD.

\* To whom correspondence should be addressed. For C.D.E.: Phone 410-455-3334; Fax 410-455-1052; Email [eggleton@umbc.edu](mailto:eggleton@umbc.edu). For M.R.M.: Phone 410-455-3439; Fax 410-455-1049; Email [marten@umbc.edu](mailto:marten@umbc.edu).

<sup>†</sup> Department of Mechanical Engineering.

<sup>‡</sup> Department of Chemical and Biochemical Engineering.

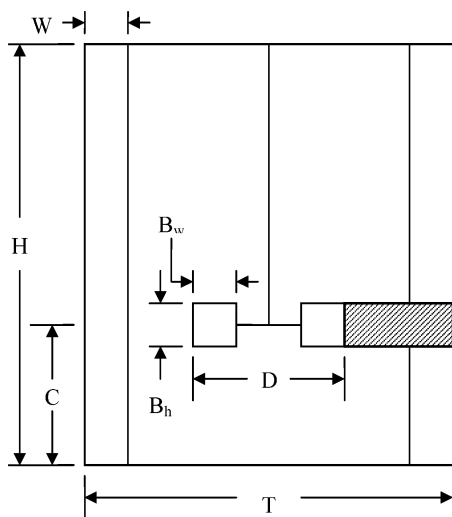


**Figure 2.** Schematic of typical single-impeller mixing tank and cross-section of circulation zone (hatched). Not drawn to scale.

A number of authors have attempted to measure the circulation time distribution in typical single-impeller mixing tanks (Figure 2). These studies are most often performed in nonaerated water or low viscosity fermentation broth and involve a flow follower technique. Middleton (8), Oosterhuis (9), and Barneveld et al. (10) employed a radio pill as the flow follower. Mukataka et al. (11), Funahashi et al. (12), and Roberts et al. (13) chose a magnet as the flow follower, and Schmitz (14) employed both. The magnet ("magnetic pill") is made neutrally buoyant, in most cases by using cork or other similar material. As for the radio pill, ballast is added or removed to achieve proper buoyancy. In both cases, to measure circulation time an antenna or inductive coil is placed in the tank at the point of reference. The radio pill transmits a signal that is received by the antenna when the pill is within a predetermined range. The motion of the magnetic pill in close proximity to the inductive coil induces a current. This fluctuating current is interpreted much like the radio signal. The signals are acquired at a predetermined sampling frequency by the data collection system, which results in a discrete signal. Data are typically collected for large numbers of circulations and processed to determine the CTD. These tests are difficult to perform and time-consuming and have yielded varying results. In addition, there is no commercial equipment available to perform these tests. Thus, a method to simply and reliably predict circulation time distribution would aid in development and scale-up or scale-down of bioreactors.

In the past, computational fluid dynamics (CFD) has been used in conjunction with experiments as a means of determining critical experimental parameters or validation of experimental results. Baldyga et al. (15) used CFD to improve theoretical model predictions of parallel chemical reactions in a continuous stirred-tank reactor. CFD results for energy dissipation rates were used to improve the qualitative agreement between a 1-D single-circulation-loop plug flow model and experimental results. Montante et al. (16) compared experimental and CFD results for solid particle distribution in a stirred tank. The authors corrected the coefficient of drag for the solid-phase calculations in CFD using empirical correlations. This correction resulted in a reported good agreement in particle concentration distribution as compared to experimental values. Bakker and van den Akker (17) compared the experimental measurements of laser dop-

pler velocimetry (LDV) with CFD predictions for three different impellers. Good agreement between the CFD predictions and experimental data were shown for axial velocity components at different axial positions in the vessel, though no quantitative values for agreement were discussed. Meng and Fox (18) validated CFD simulations of stirred tanks using particle image velocimetry (PIV) data. The axial and radial components of velocity were compared with the PIV data for several axial positions. The CFD values for axial velocity were  $\pm 10\%$  of the PIV values; in the impeller flow and discharge regions, the error reduced to  $\pm 5\%$ . For the radial component of the velocity, good agreement was found in the upper region of the tank whereas some error was seen in the discharge and return regions. Despite the errors found, CFD captured the important characteristics of the mean flow pattern. Jaworski, Dyster, and Niewnow (19) compared CFD predictions with laser doppler anemometry (LDA) measurements of pitched-blade turbines. Close agreements between the predictive and experimental values for mean flow were found with the exception of some small regions. Large differences were obtained in turbulence parameters; however, the authors determined that the ability of CFD to generate rather accurate mean flow patterns represents an effective method for optimizing impeller-tank designs for particular process results.

The goal of this study was to take a first step toward the prediction of CTD in a fermentor by determining whether currently available CFD software could be used to estimate the CTD in a nonaerated, single-impeller mixing tank. Three published tank geometries and operating conditions (8, 13, 14) were used as input for FLUENT/MixSim CFD software. FLUENT simulated the time-averaged turbulent flow fields in the tanks. Tracer particles were released from a reference zone, and the circulation times for each of the particles was determined. Results of the simulations were compared to measured CTDs for all three tanks. The ability of CFD to predict the CTD is reported, and improved methods for experimentally determining CTDs are discussed.

## Materials and Methods

**Experimental Measurements of Circulation Time Distribution (CTD).** In experimental studies taken from the literature (8, 13, 14) and used here, the flow follower technique was employed in single-impeller (6-blade, Rushton turbine) mixing tanks (Figure 2), with similar geometric features and operating conditions (Table 1), using water at room temperature. Middleton (8) and Roberts et al. (13) used a magnetic pill, whereas Schmitz (14) used a radio pill as the neutrally buoyant flow follower to make circulation measurements. This was accomplished by placing a detector (induction coil or antenna) around the tank at the impeller height, creating a reference zone. In all three cases, the detector generated a signal as a result of the flow follower entering the reference zone. This signal was discretely sampled and recorded by the data collection system. The output data collected consisted of a discrete time resulting from the particle being within the reference zone at the particular instant when the inductor/antenna signal was sampled. All three authors used different sampling frequencies ( $t_s$ ) for data collection (Table 2). The time of the current pulse was recorded and the time between two consecutive pulses indicated one circulation. A large number of circulation times were collected (Table 2), and the CTD for the tank was generated.

**Table 1. Mixing Tank Dimensions (Figure 2) with Experimental Study Parameters**

parameter	symbol	units	tank 1 Middleton (8)	tank 2 Roberts et al. (13)	tank 3 Schmitz (14)
volume	$V$	$m^3$	0.598	0.011	0.293
tank diameter	$T$	m	0.915	0.240	0.720
liquid height	$H$	m	0.910	0.240	0.720
liquid height			$H = T$	$H = T$	$H = T$
impeller speed	$N$	rev $s^{-1}$	7.5	4.17	5.0
impeller diameter	$D$	m	0.303	0.080	0.240
impeller diameter			$D = T/3$	$D = T/2$	$D = T/3$
Reynolds number	$N_{Re}$		688,567	26,688	288,000
off-bottom clearance	$C$	m	0.303	0.120	0.240
off-bottom clearance			$C = T/3$	$C = T/2$	$C = T/3$
number of baffles			4	4	4
baffle width	$W$	m	0.091	0.024	0.072
baffle width			$W = T/10$	$W = T/10$	$W = T/10$
blade width	$B_w$	m	0.076	0.020	0.060
blade width			$B_w = D/4$	$B_w = D/4$	$B_w = D/4$
blade height	$B_h$	m	0.061	0.016	0.060
blade height			$B_h = D/5$	$B_h = D/5$	$B_h = D/4$
flow follower			magnetic	magnetic	radio
experimental fluid			water	water	water
reference zone			impeller	impeller	impeller

**Table 2. Sampling Frequencies for Experimental CTD and Approximate Experimental Circulations**

author	sampling frequency $t_s$ (s)	approximate circulations
Middleton (8)	0.3	1000
Roberts et al. (13)	0.145	4000
Schmitz (14)	0.1	2000

**Computational Fluid Dynamics (CFD) Software Simulation.** Three single-impeller mixing tanks (Figure 2) with associated operating conditions (Table 1) that have been used for experimental CTD determination (8, 13, 14) were used for CFD simulations. All simulations were performed using FLUENT 4 (V4.56, Fluent, Lebanon, NH) on a single Sparc 2 CPU (Sun Microsystems) rated at 300 MHz with 1.2 GB of available RAM. MixSim software (Fluent, Lebanon, NH) was used to create the geometry of the mixing tanks detailed in Table 1. Subsequently, FLUENT 4 was used to solve the Navier–Stokes equations to obtain the flow field inside the mixing tanks.

A three-dimensional model was chosen to represent tank geometry. Note that although a wedge of the tank could have been used to calculate the flow field, the entire geometry of the tank is modeled to facilitate the calculation of the tracer particle trajectories. The dimensions of this model extended axially from the liquid surface to the tank bottom ( $z$ ), radially from the centerline to the tank wall ( $r$ ), and around the circumference of the tank ( $\theta$ ). The grid is constructed so as to conform to the shapes of the objects inside the tank. The grid is not entirely uniform but gradually varies from one region of the tank to another in order to ensure smooth grid transitions. The meshing was similar for each of the three tanks. The number of elements in the three coordinates ( $z$ ,  $r$ ,  $\theta$ ) were 194, 32, 61 for Tank 1; 194, 32, 62 for Tank 2; and 193, 31, 62 for Tank 3. To calculate the flow field, FLUENT models flows as turbulent in mixing tanks with Reynolds number greater than 2,000 (20). The flow field inside a mixed tank will depend on the flow regime (turbulent or laminar) as described by the Reynolds number ( $N_{Re} = \rho ND^2/\mu$ ). For simulations performed here,  $N_{Re}$  was determined using values of density ( $\rho = 1000 \text{ kg m}^{-3}$ ) and viscosity ( $\mu = 0.001 \text{ kg m}^{-1} \text{ s}^{-1}$ ) where  $N$  is in revolutions per second and  $D$  is the impeller diameter consistent with experiments. In all tanks, the Reynolds number was found to be  $>2000$ , or fully turbulent (Table 1) (21).

The  $\kappa$ - $\epsilon$  turbulence model described by Ferziger (22) was used to solve for time-average turbulent conditions inside the tanks. Although turbulent flow is inherently unsteady, the  $\kappa$ - $\epsilon$  turbulence model predicts the time-averaged viscous stresses, allowing time-averaged steady solutions to be calculated. FLUENT software was used to solve the governing equations for the conservation of mass and momentum by reducing them to their finite-volume analogues, using a semi-implicit iterative scheme. Starting from quiescent initial conditions (except at the boundaries), the equations are marched through time until converging to the steady-state solution (23). For each iteration, the momentum equations are solved using current values for pressure, to update the velocity field. The  $\kappa$  and  $\epsilon$  equations are solved using the previously updated values of the other variables. The fluid velocities are then updated, and a check for convergence of the system of equations is made. The steady-state solution is reached when the change in all of the calculated variables is less than a chosen tolerance of  $1 \times 10^{-5}$ . The rotation of the impeller at constant angular velocity was accounted for using a multireference frame scheme (23).

**CFD Simulation for Prediction of Circulation Time Distribution.** Having obtained the time-averaged steady flow field inside the mixing tank, neutrally buoyant tracer particles were released in the tank in order to calculate their trajectories and determine the distribution of circulation times. The reference zone used to calculate circulation time is given by the hatched area in Figure 2. The cross-section extends radially from the edge of the blade to the tank wall, axially along the height of the blade and extended throughout the circumference of the tank. This zone is similar but not identical to the regions chosen for all three experimental measurements because no definitive coordinates are given in the literature. Initial release points for all of the particles were within the reference zone. A large number of particles were released in each of the three tanks. These particles were evenly distributed along the  $r$  and  $z$  directions of the reference zone. The even distribution of tracer particles continued for  $90^\circ$  in the  $\theta$  direction. This “wedge” of particles was positioned in the  $\theta$  direction so as to have a baffle located at the midline of the distribution of particles in the  $\theta$  direction. This wedge position would allow for the maximum number of unique trajectories. The release pattern was chosen to ensure the particles were subjected to possible three-dimensional

variations in the flow field. The variations may include tangential dependence of the centers of the two main circulation loops that dominate the flow (17).

The numbers of particles released for each tank were as follows: Tank 1, 5175; Tank 2, 3420; and Tank 3, 5700. These particles were released into the flow field, and their positions were tracked over a period of 30 s. A particle's trajectory is predicted by balancing inertia with other forces (i.e., drag force). The force balance is integrated to determine the particle velocity. The smallest integral time step allowed by the software is 0.01 s. Some of the particles encountered solid boundaries of the tank wall or impeller in the calculated path. Consequently, the path of the tracer particle was blocked, and further tracking was terminated. The stored data consisted of the axial, radial, and azimuthal location of the particle at the various time steps, in addition to the velocity magnitudes in the three coordinate axes.

The data resulting from the particle releases was converted to a discrete signal, at the appropriate sampling frequency for each tank, to match the experimental signals. The simulated signal consisted of a marker indicating that the particle is in the reference zone along with the particle number and associated time step (similar to the signal received by the experimental data collection systems). The simulated data signal was processed such that the circulation time was the difference between two consecutive "in-markers" for each individual particle, similar to the processing of the experimental signal (8, 13, 14). The CTD was calculated by distributing the circulations completed by each particle in 30 s into specified time bins, summing the number of circulations in a time bin, and dividing the total in each bin by the total number of circulations. The bins are ranges of circulation times. For each tank, the bin sizes were chosen to match the experimental bin sizes: Middleton (8), 1.0 s; Roberts et al. (13), 0.10 s; Schmitz (14), 0.10 s.

## Results and Discussion

The methods described above were used to recreate experimentally measured CTDs using CFD software. The three tank geometries were created and meshed using MixSim. Boundary and operating conditions were specified, and the time-averaged steady flow field was solved using the  $\kappa$ - $\epsilon$  turbulence model in FLUENT. Tracer particles were then released into the flow field, and the trajectories were tracked by the software. These particle trajectories were used to determine the CTD for each of the tanks. The time required for tracking all particles was a function of the number of particles and time step chosen to advance particle tracking. For a time step of 0.01 s and 5000 particles, approximately 200 h were required to determine all trajectories. The trajectories were used to create a simulated signal at the appropriate sampling frequency ( $t_s$ ). This signal was then processed using the same methods employed in the experiments to determine the CTD (8, 13, 14).

CTDs measured in the three tanks are compared with the CTDs determined via CFD simulation in Figure 3. In each of the three cases, the dashed line indicates experimentally determined CTD, and the solid line indicates CTD determined via CFD. A qualitative comparison of the measured and simulated CTDs shows that the CFD simulation is able to capture the distinguishing features in the probability distributions. For Tank 1, the 5175 released particles resulted in 9053 circulations, versus 1000 circulations in the experimental determina-

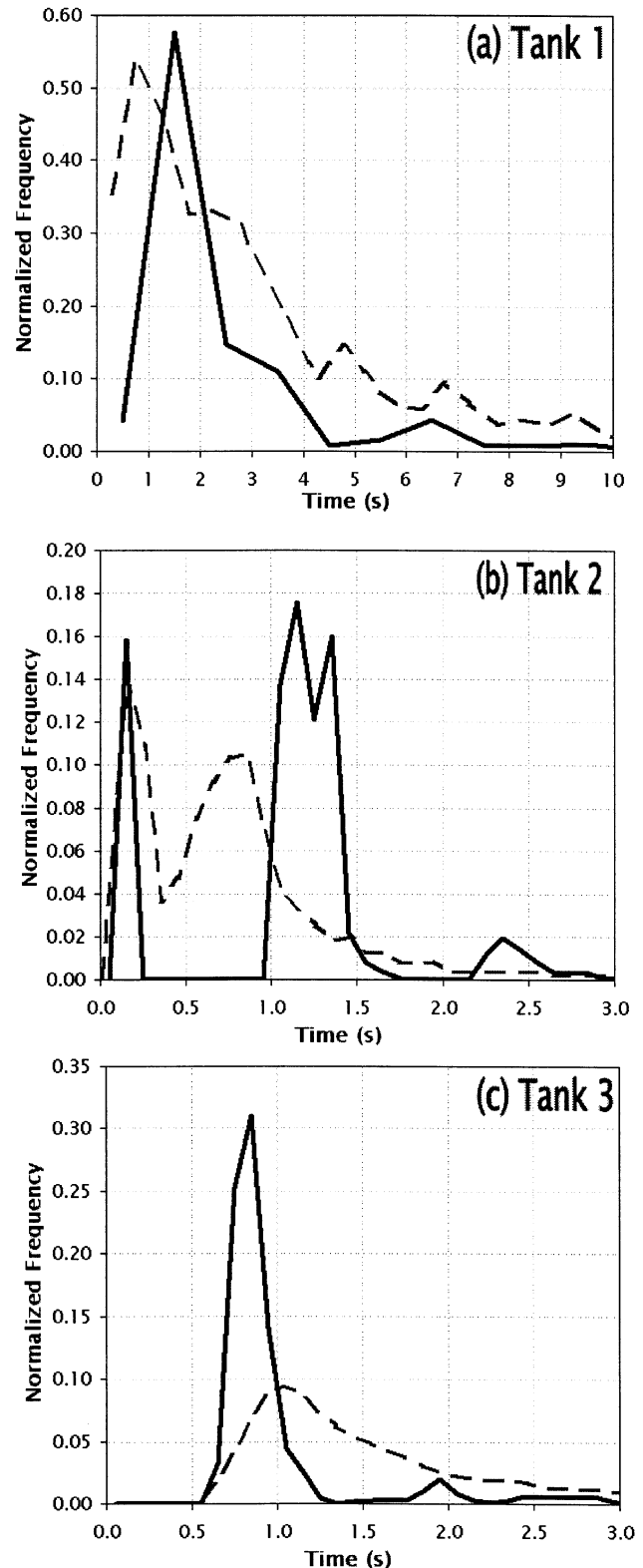


**Figure 3.** Experimental (---) and simulated (—) circulation time distributions for Tanks 1–3 described in Table 1.

tion of the CTD (8). In Figure 3a both curves show a unimodal, log-normal type of distribution of the probability function with a good qualitative agreement between experimental and simulated CTD. For Tank 2, the 3420 released tracer particles resulted in 9005 circulations, versus 4000 circulations in the experimental determination of the CTD (13). Although the peaks do not coincide, the simulated CTD qualitatively captures the

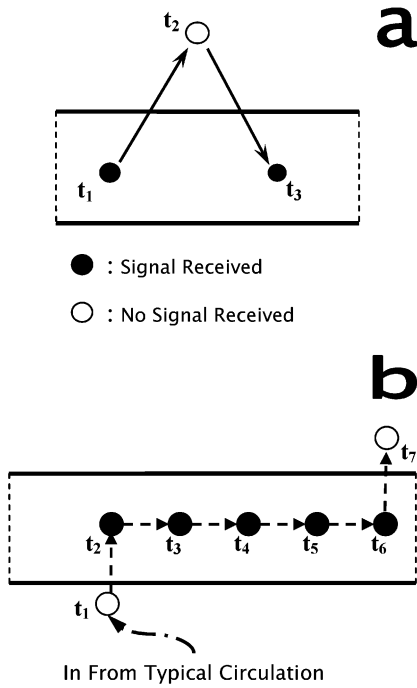


**Figure 4.** (a) Schematic of shortest circulation where  $t_3 - t_2 = t_2 - t_1 = t_s$  (i.e., sampling frequency). The shortest circulation is  $2t_s$ . (b) Hypothetical particle trajectory through the reference zone where  $t_2 - t_1 = t_3 - t_2 = t_4 - t_3 = t_5 - t_4 = t_6 - t_5 = t_7 - t_6 = t_s$ .

bimodal nature of the experimentally determined CTD (Figure 3b). In Tank 3, 5700 tracer particles were released into the flow field, resulting in 14358 circulations, versus 2000 circulations in the experimental determination of the CTD (14). Again, the simulated CTD qualitatively captures the unimodal behavior of the experimentally determined CTD (Figure 3c).

For Figure 3, differences in the positions of the maxima of the CTD may be due to differences in the size, shape, and exact locations of the reference zones that were not fully described in the literature. Differences in the variances of each peak may come from using the time-averaged flow field, which does not allow for the proba-

bilistic nature of turbulent flow. The CFD simulation involves only a finite number of streamlines. In reality, the stochastic nature of turbulent flow will result in many more trajectories than exist in the CFD time-averaged flow field. These additional trajectories are likely responsible for the relative smoothness of the experimentally measured CTD curves.

We note that all three tanks are similar in geometry, and thus it is not unreasonable to expect the CTDs to have similar shape; yet they do not. Our simulations imply that signal processing may be the source for the various shapes. For example, the bimodal shape of the CTD for Tank 2 (Figure 3b) may be the result of recording false circulations. For any given circulation, the difference between the times the particle moves out of and re-enters the reference zone determines the circulation time,  $t_c$ . Therefore, the shortest possible circulation time depends on the sampling frequency used in the experiment. Figure 4a shows that the shortest circulation time that can be measured or resolved is double the sampling frequency,  $2t_s$ . Thus, it is experimentally impossible to measure circulation times  $t_c < 2t_s$ . For measurements in Tank 2,  $t_s$  was given as 0.145 s (Table 2) yet Figure 3b shows a CTD peak in the 0.1–0.2 s bin. Thus, it seems likely that the circulations associated with the first peak in Figure 3b were due to the particle moving through the reference zone causing multiple triggering of the data collection system, which was misinterpreted as multiple circulations. In Figure 3c, the experimental peak that would be associated with multiple triggering of the data collection system is not present because experimental circulations of less than 0.5 s were disregarded (14). For Figure 3a, the relatively low sampling frequency of 0.3 s (Table 2) and large bin size of 1.0 s (8) reduced the magnitude of the multiple triggering peak with respect to the largest peak in the second bin (1.0–2.0 s), where CFD predicts a majority of the real circulations reside.

To explain the idea of multiple triggering, Figure 4b shows a hypothetical particle trajectory within the reference zone. The particle re-enters the reference zone following a typical particle trajectory (Figure 5). The particle then travels through the reference zone following the velocity vectors of the time-averaged flow field (Figure 6). The particle moves along the direction of the velocity

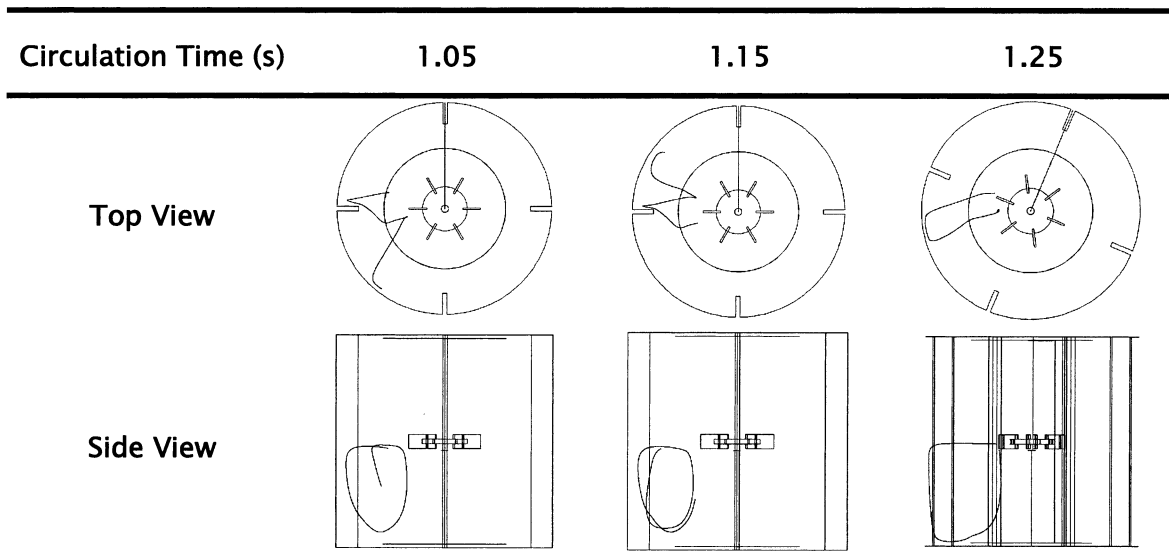


**Figure 5.** Typical particle trajectories with associated circulation time. Top view shows the radial and tangential trajectories of the particle paths. Side view shows the radial and axial trajectories of the particle paths.

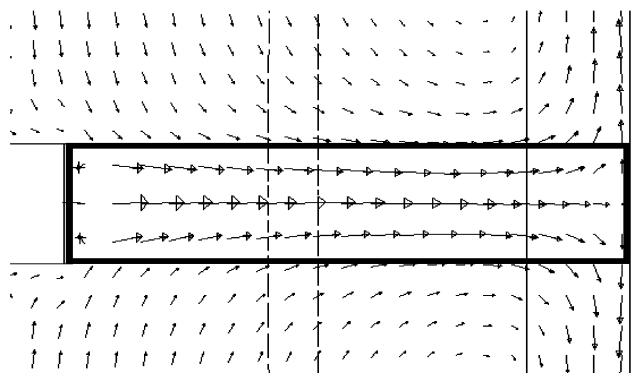


**Figure 6.** Velocity vectors in radial jet of impeller with reference zone superimposed (—).

vector with zero probability of changing streamlines. The particle tracks obtained via CFD then travel to the tank wall and into the two main circulation loops dominating the flow (17). Experimentally, the circulation time would be the difference between two consecutive pulses of the data collection system (8, 13, 14). The particle trajectory shown in Figure 4b would result in multiple short circulations with  $t_c = t_s$ . We know that the shortest circulation time possible is  $2t_s$ ; therefore, these circulations must be disregarded because the particle never left and re-entered the reference zone.

Utilizing CFD allows for inspection of the simulated particle tracks along with the 3-D position of all particles at 0.01 s time steps. Using the simulated trajectories, the first time step in which a particular particle left the geometric bounds of the reference zone was stored as the exit time. The particle's position was followed. When a particle is observed to re-enter the reference zone, the entry time is recorded. A calculated circulation time is the entry time minus the exit time. The same simulated particle trajectories used to create the predicted CTDs in Figure 3 are now processed as described above. Circulation times are sorted into 0.1 s bins for all three tanks, and each bin is normalized by the total number of circulations recorded for each simulation. As a result of the new analysis, the numbers of circulations recorded are 13616, 9729, and 14910 for Tanks 1, 2, and 3, respectively. The increase in total circulations is due to the increased temporal resolution of trajectory data. Previously the resolution was 0.3, 0.145, and 0.1 s for Tanks 1, 2, and 3, respectively. The results of the new analysis of the particle trajectories are shown in Figure 7. As might be expected for the three similar single-impeller mixing tanks, the CTDs have similar unimodal distributions.

### Conclusions

Computational Fluid Dynamics qualitatively captured the distinguishing features of the experimental CTDs for three single-impeller mixing tanks. It was found that current methods for processing experimental signals may result in inaccurate probability distributions. Simple analysis shows the shortest circulation time that can be resolved is double the sampling frequency but that current signal processing methods can result in multiple circulation times less than double the sampling frequency as the flow follower passes through the reference zone. CFD provides the ability to determine the circulation time based on position of the particle, therefore eliminating circulation times due to multiple triggering. When

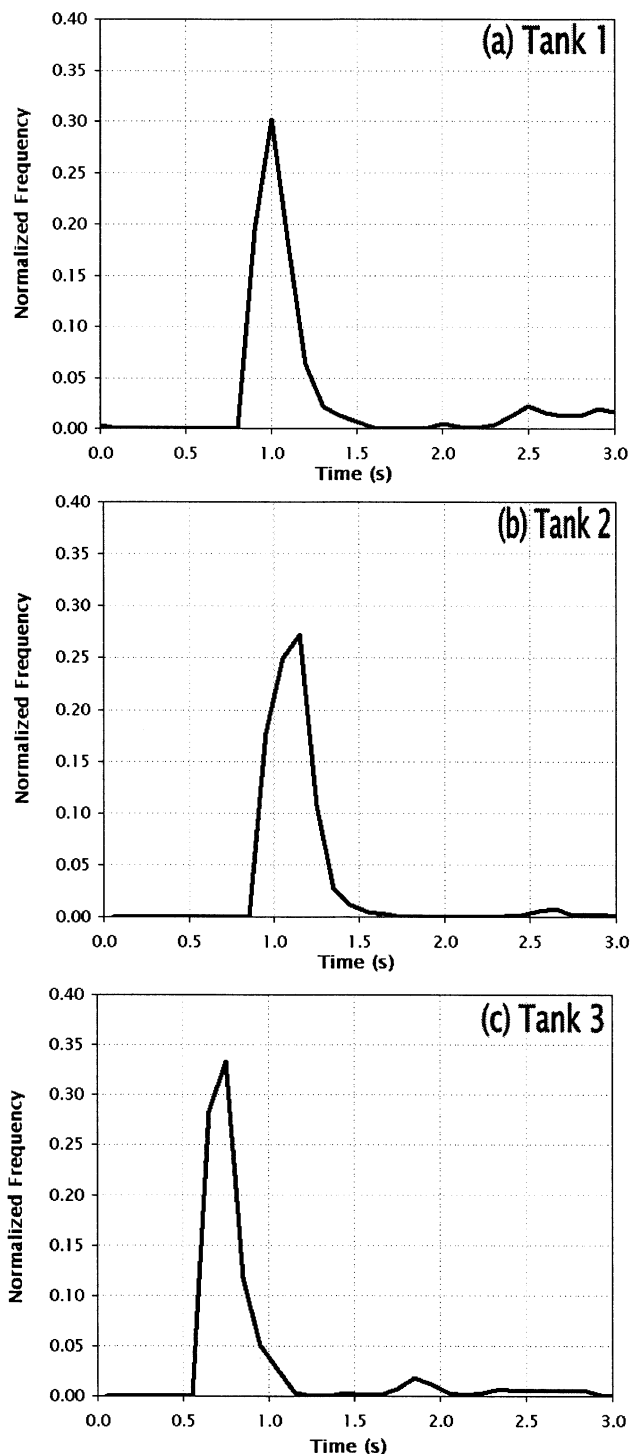


**Figure 7.** Simulated circulation time distribution for Tanks 1–3 described in Table 1.

this was taken into account, CFD simulations resulted in similar unimodal CTDs for tanks with similar geometries.

### References and Notes

- (1) Bryant, J. The characterization of mixing in fermentors. *Adv. Biochem. Eng.* **1977**, *5*, 101–123.
- (2) Namdev, P. K.; Yegneswaran, P. K.; Thompson, B. G.; Gray, M. R. Experimental simulation of large-scale bioreactor environments using a Monte Carlo method. *Can. J. Chem. Eng.* **1991**, *69*, 513–519.
- (3) Li, Z. J.; Shukla, V.; Pedersen, A. G.; Wenger, K. S.; Fordyce, A. P.; Marten, M. R. Effects of increased impeller power in a

- production-scale *Aspergillus oryzae* fermentation. *Biotechnol. Prog.* **2002**, *18*, 437–444.
- (4) Marten, M. R.; Wenger, K. S.; Khan, S. A. Rheology, mixing time, and regime analysis for a production-scale *Aspergillus oryzae* fermentation. In *Bioreactor and Bioprocess Fluid Dynamics*; Nienow, A. W., Ed.; BHR Group: Cranfield, UK, 1997; pp 295–313.
  - (5) Bylund, F.; Collet, E.; Enfors, S. O.; Larsson, G. Substrate gradient formation in the large-scale bioreactor lowers cell yield and increases byproduct formation. *Bioprocess Eng.* **1998**, *18*, 171–180.
  - (6) Namdev, P. K.; Thompson, B. G.; Gray, M. R. Effect of feed zone in fed-batch fermentations of *Saccharomyces cerevisiae*. *Biotechnol. Bioeng.* **1992**, *40*, 235–246.
  - (7) Mann, U.; Crosby, E. J. Cycle time distribution in circulating systems. *Chem. Eng. Sci.* **1973**, *28*, 623–627.
  - (8) Middleton, J. C. Measurement of circulation within large mixing vessels. *Third European Conference on Mixing*, 1979, York, UK; Paper A, pp 15–36.
  - (9) Oosterhuis, N. M. G. Scale up of bioreactors, a scale down approach, Ph.D. Thesis, Delft University of Technology, The Netherlands, 1984.
  - (10) Barneveld, J. v.; Smit, W.; Oosterhuis, N. M. G.; Pragt, H. J. Measuring the liquid circulation time in a large gas–liquid contactor by means of a radio pill. 2. Circulation time distribution. *Ind. Eng. Chem. Res.* **1987**, *26*, 2192–2195.
  - (11) Mukataka, S.; Kataoka, H.; Takahashi, J. Circulation time degree of fluid exchange between upper and lower circulation regions in a stirred vessel with a dual impeller. *J. Ferment. Technol.* **1981**, *59*, 303–307.
  - (12) Funahashi, H.; Harada, H.; Taguchi, H.; Yoshida, T. Circulation time distribution and volume of mixing regions in highly viscous xanthan gum solution in a stirred vessel. *J. Chem. Eng. Jpn.* **1987**, *20*, 277–282.
  - (13) Roberts, R. M.; Gray, M. R.; Thompson, B.; Kresta, S. M. The effect of impeller and tank geometry on circulation time distributions in stirred tanks. *Trans. Inst. Chem. Eng.* **1995**, *73A*, 78–86.
  - (14) Schmitz, R. Circulation time studies in newtonian and nonnewtonian fluids in stirred tanks. Ph.D. Thesis, University of Birmingham, UK, 1996.
  - (15) Baldyga, J.; Henczka, M.; Makowski, L. Effects of mixing on parallel chemical reactions in a continuous-flow stirred-tank reactor. *Trans. Inst. Chem. Eng.* **2001**, *79A*, 895–900.
  - (16) Montante, G.; Micale, G.; Magelli, F.; Brucato, A. Experiments and CFD predictions of solid particle distribution in a vessel agitated with four pitched blade turbines. *Trans. Inst. Chem. Eng.* **2001**, *79A*, 1005–1010.
  - (17) Bakker, A.; Van den Akker, H. E. A. Single phase flow in stirred reactors. *Trans. Inst. Chem. Eng.* **1994**, *72A*, 583–593.
  - (18) Meng, J. S.; Fox, R. O. Validation of CFD simulations of a stirred tank using particle image velocimetry data. *Can. J. Chem. Eng.* **1998**, *76*, 611–625.
  - (19) Jaworski, Z.; Dyster, K. N.; Nienow, A. W. The effect of size, location and pumping direction of pitched blade turbine impellers on flow patterns: LDA measurements and CFD predictions. *Trans. Inst. Chem. Eng.* **2001**, *79A*, 887–893.
  - (20) Fluent Incorporated. *MixSim User's Guide*. Fluent Inc: Lebanon, NH, 1998.
  - (21) Nienow, A. W. Hydrodynamics of stirred bioreactors. *Appl. Mech. Rev.* **1998**, *51*, 3–31.
  - (22) Ferziger, J. H.; Perić, M. *Computational Methods for Fluid Dynamics*; Springer: New York, 1997; pp 271–282.
  - (23) *FLUENT Manual*; Fluent Inc.: Lebanon, NH, 1997.

Accepted for publication July 2, 2003.

BP025580D